

EXPERIMENTAL AND THEORETICAL STUDY OF BIRCH ETHANOL LIGNIN HYDROGENATION PRODUCTS ON RU/C CATALYST

ALEKSANDR S. KAZACHENKO,^{*,**} FERIDE AKMAN,^{***} ANGELINA MIROSHNIKOVA,^{*,**}
ANDREY SKRIPNIKOV,^{*,**} XIAOMIN LI,^{*} VALENTIN V. SYCHEV,^{*,**} O. S. SELEZNEVA,^{**}
UTKIRJON HOLIKULOV,^{***} NOUREDDINE ISSAOU,^{****} and OMAR M. AL-DOSSARY^{*****}

^{*}*Siberian Federal University, pr. Svobodny 79, Krasnoyarsk, 660041 Russia*

^{**}*Institute of Chemistry and Chemical Technology, Krasnoyarsk Scientific Center, Siberian Branch, Russian Academy of Sciences, Akademgorodok 50, bld. 24, Krasnoyarsk, 660036 Russia*

^{***}*Vocational School of Food, Agriculture and Livestock, University of Bingöl, Bingöl 12000, Turkey*

^{****}*Department of Optics and Spectroscopy, Samarkand State University, 15 University Blvd., Samarkand, 140104 Uzbekistan*

^{*****}*Laboratory of Quantum and Statistical Physics, Faculty of Sciences, University Monastir, 5079 Tunisia*

^{*****}*Department of Physics and Astronomy, College of Science, King Saud University, PO Box 2455, Riyadh, 11451 Saudi Arabia*

✉ *Corresponding author: A. S. Kazachenko, kazachenko.as@icct.krasn.ru*

Received April 3, 2024

Plant biomass is a valuable raw material for the production of important chemicals. Lignin depolymerization processes make it possible to obtain valuable aromatic substances. In this work, the aromatic products of birch ethanol lignin hydrogenation were studied. The lignin depolymerization process was carried out on a ruthenium catalyst, varying the oxidation temperature of the carbon carrier. The hydrogenation products were analyzed by GC, GC-MS and DFT. It was shown that the highest yield of monomeric methoxyphenols (about 11 wt%) was achieved using the 3% Ru/C(400) catalyst. Catalysts have a significant effect on the yield and composition of solid, liquid and gaseous products. Thus, the use of the most effective 3% Ru/C(400) catalyst increased the yield of monomeric methoxyphenols from 2.2 to 11.1 wt% compared to the non-catalytic experiment. The liquid products of birch ethanol lignin hydrogenation mainly consist of syringol derivatives, which were studied using density functional theory methods. Spectroscopic (FTIR and NMR) characteristics, HOMO-LUMO, Mulliken atomic charges, electronic parameters, MEP and ALIE were calculated. Optical softness, softness and maximum charge transfer index values increased with increasing chain length of the alkyl radical and the appearance of a double bond.

Keywords: lignin, hydrogenation, ethanol, DFT, biomass

INTRODUCTION

Recently, the use of renewable plant biomass instead of fossil resources has attracted increasing attention from researchers as a sustainable alternative to the modern petrochemical industry.¹ Wood is a widespread and accessible source of biomass, considered as a raw material for the production of a variety of chemical products. The main structural components of wood are interconnected into a complex rigid matrix and thermal and solvolytic processing is required for its selective transformation into products with high added value.^{1,2} A well-known method for isolating lignin is the extraction of lignocellulosic

raw materials with low-boiling organic solvents or their mixtures with water at temperatures of 180–200 °C.³ The resulting organosolv lignins, unlike traditional technical ones, do not contain sulfur, which reduces the efficiency of thermocatalytic processing, and have high reactivity in the temperature range of 250–400 °C. Effective depolymerization of lignin can be achieved by thermal conversion in lower aliphatic alcohols in a supercritical state.⁴ It is known that the use of supercritical fluids in “green” chemistry processes makes it possible to increase the yield of extracted products.⁵ The choice of alcohols is due to the fact

that their critical temperatures are lower or close to the region of optimal temperatures for the thermal destruction of lignin. To increase lignin conversion and the yield of monomer products, solid acid catalysts, such as zeolites, as well as Ni, Mo, Co and platinum group metals on various supports, are often used.^{6,7}

In this work, a comprehensive comparative study of monomeric hydrogenation products of birch ethanol lignin obtained on a Ru/C catalyst with different characteristics of the catalyst support was carried out. The main products of hydrogenation of birch ethanol lignin were studied using theoretical methods. The Ru/C catalyst based on oxidized Sibunit showed good catalytic properties in the depolymerization and hydrogenolysis of various types of lignin.^{8,9}

EXPERIMENTAL

The extraction of ethanol lignin from wood was carried out by extraction with an ethanol-water mixture at a temperature of 185 °C and subsequent precipitation with cold water according to a previously described method.¹⁰

Method for obtaining the catalyst

The catalyst was prepared on a graphite-like carbon support Sibunit-4® ground in a porcelain mortar. A fraction with a particle size of 56–96 µm was used. The carrier was oxidized with humid air for 4 hours at 450 °C. A catalyst containing 1% ruthenium was prepared by impregnating a carbon support according to its moisture capacity with an aqueous solution of ruthenium nitrasyl nitrate, followed by reduction in hydrogen.¹¹ The characteristics of the catalysts are shown in Table 1.

Table 1
Texture and acid characteristics of carbon support and supported ruthenium catalysts (3 wt% Ru)

Catalyst	Oxidation temperature of support, °C	BET surface area (S_{BET}), m^2/g	Pore volume (V_{pore}), cm^3/g	Average pore size ($\langle d_{\text{pore}} \rangle$), nm	pH_{pzc}^*
3%Ru/Sib-4	without oxidation	273	0.32	4.77	8.05
3%RuS400	400	300	0.37	5.01	7.12
3%RuS450	450	341	0.50	5.88	6.89

* pH_{pzc} is the pH of the point of zero charge

Hydrogenation of birch ethanol lignin

The hydrogenation process was carried out in a ChemRe SYSTEM R-201 autoclave (Korea) with a volume of 300 mL. The reactor was loaded with 50 mL of ethanol, 5.0 g of substrate and 0.5 g of catalyst. Then, the autoclave was hermetically sealed and purged with argon to remove air. Hydrogen was supplied, the initial pressure of which was 3 MPa. The reaction was carried out with constant stirring at a speed of 1000 rpm, at a temperature of 300 °C for 1 hour. The rate of temperature rise was 10 °C/min, the time to reach the required temperature was 20–25 minutes. The operating pressure in the reactor was 9.0 MPa. After cooling the reaction mixture to room temperature, the gaseous products were collected in a gasometer, their volume was measured, and the composition was determined by gas chromatography. Then, the reaction products were quantitatively discharged from the autoclave by washing with ethanol, and the resulting mixture of liquid and solid products was separated by filtration.

The solid was washed with ethanol until the solvent became colorless. The solvent was removed from the liquid product using a rotary evaporator, and the product was brought to constant weight by drying under vacuum (1 mm Hg) at room temperature. The solid product was dried at a temperature of 80 °C to

constant weight. The yield of liquid products (α_1), the yield of solid product (α_2), the total yield of gaseous products (α_3) and the degree of lignin conversion (χ_1) were determined using Equations (1–4):

$$\alpha_1 = \frac{m_l (g)}{m_i (g)} \times 100\% \quad (1)$$

$$\alpha_2 = \frac{m_s (g) - m_{\text{cat}} (g)}{m_i (g)} \times 100\% \quad (2)$$

$$\alpha_3 = \frac{m_g (g)}{m_i (g)} \times 100\% \quad (3)$$

$$\chi_1 = \frac{m_l (g) + m_{\text{cat}} (g) - m_s (g)}{m_i (g)} \times 100\% \quad (4)$$

where χ_1 – conversion of ethanol lignin, %; m_l – mass of liquid products (g), m_i – mass of the original sample (g), m_{cat} – catalyst mass (g), m_g – mass of gaseous products (g), m_s – mass of solid residue.

Study of hydrogenation products of birch wood ethanol lignin

The composition of gaseous products of the thermal transformation of ethanol lignin in supercritical ethanol was determined by GC on a Kristall 2000 M chromatograph (Chromatek, Russia), with a thermal conductivity detector. The carrier gas was helium (flow rate of 15 mL/min); detector temperature: 170 °C. To

analyze CO and CH₄, a column with NaX zeolite (3 m × 2 mm) was used in isothermal mode at a temperature of 60 °C. The analysis of CO₂ and hydrocarbon gases was carried out on a column with Porapak Q in the mode: 1 min – 60 °C, and then increasing the temperature to 180 °C at a rate of 10 °C/min.

Ethanol soluble liquid products were GC-MS analyzed using an Agilent 7890A chromatograph, equipped with an Agilent 7000A TripleQuad detector of selective masses at recording the total ion current. Products were separated using a capillary column HP-5MS at temperature programmed between 40 and 250 °C. Products were identified using the NIST MS Search 2.0 database.

Calculation details

The DFT/B3LYP and 6-311++G(d,p) methods were used to optimize the molecular structures of syringol and its derivatives. The programs Gaussian09W¹² and GaussView5.0¹³ were utilized to carry out all the necessary DFT calculations and visualizations.

RESULTS AND DISCUSSION

Hydrogenation of birch ethanol lignin

In the process of non-catalytic hydrogenation, the conversion of birch ethanol lignin in supercritical ethanol at 300 °C reaches 75.2 wt% (Fig. 1). In the presence of ruthenium-containing catalysts, the conversion of birch ethanol lignin

increases to 98.9 wt%. The bifunctional catalyst 3%Ru/C (400) exhibits higher activity. The conversion of birch ethanol lignin in its presence is 98.9 wt%.

In the presence of catalysts, the yield of liquid products formed during the hydrogenation of birch ethanol lignin at a temperature of 300 °C increases noticeably (Table 2). In the process of non-catalytic hydrogenation of birch ethanol lignin, the content of liquid and solid products is 63.0 and 24.8 wt%, respectively.

The use of ruthenium-containing catalysts leads to an increase in the yield of liquid products to 82.8 wt% and a decrease in the yield of solid products to 1.1 wt%. The maximum content of liquid products (82.8 wt%) is observed when using a 3%Ru/C (450) catalyst. The minimum solids content (1.1 wt%) is observed when using a 3%Ru/C (400) catalyst.

The composition of the gaseous products of ethanol lignin hydrogenation consists mainly of methane, as well as carbon dioxide and carbon monoxide; ethane and alkanes with higher molecular weights are found in trace amounts.⁸

Catalysts also help to increase the yield of gaseous products (Table 2). The most intense gas formation is observed in the case of the catalyst 3%Ru/C (400) – with 25.6 wt% at 300 °C.

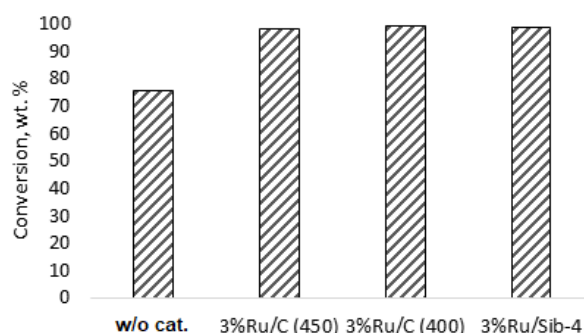


Figure 1: Effect of catalysts on the conversion of birch ethanol lignin during its hydrogenation in supercritical ethanol at 300 °C

Table 2

Yields of hydrogenation products of birch ethanol lignin with hydrogen in supercritical ethanol in the presence of ruthenium-containing catalysts (300 °C, 1 hour, initial hydrogen pressure 3.0 MPa)

Catalyst	Yield of products, wt%			Residue, %
	Liquid	Solid	Gas	
W/o	63.0	24.8	11.4	0.8
3%Ru/C (450)*	82.8	1.9	13.1	2.2
3%Ru/C (400)*	73.3	1.1	19.5	6.1
3%Ru/Sib-4**	75.3	1.6	20.0	3.1

* The oxidation temperature of the carrier during catalyst preparation is given in parentheses;

** Oxidation of the carrier was not carried out

Table 3

Composition of liquid products of non-catalytic and catalytic hydrogenation of birch ethanol lignin according to GC-MS data (conditions: 300 °C, 1 hour, initial hydrogen pressure 3.0 MPa)

RT	Substance	W/o cat.	3%Ru/C (450)	3%Ru/C (400)	3%Ru/ Sib-4
17.94	Guaiacol	0.06	0.25	0.53	0.41
20.78	4-ethylphenol	-	0.09	-	0.04
21.51	4-methylguaiacol	0.17	0.30	0.53	0.49
23.63	3-methoxycatechin	-	0.18	0.30	0.03
24.15	4-ethylphenol	0.07	0.16	0.28	0.33
26.23	Siringol	0.61	1.11	2.26	1.83
26.64	4-propylguaiacol	0.09	0.38	0.58	0.61
28.76	4-methylsyringol	0.58	1.08	1.86	1.59
29.26	Coniferyl alcohol	-	0.04	0.05	-
30.724	4-ethylsyringol	0.15	0.45	0.78	0.67
32.74	4-propylsyringol	0.46	2.09	3.21	3.14
34.02	4-propenylsyringol	0.05	0.06	0.12	0.07
35.47	Ethanone, 1-(4-hydroxy-3,5-dimethoxyphenyl)	-	0.09	0.15	-
36.27	Syringylacetone	-	0.10	0.18	0.05
37.38	Propiosyringone	-	0.09	0.13	-
38.76	Propanolsyringol	-	0.30	0.19	-
Total yield of methoxyphenols		2.24	6.77	11.15	9.26

Analysis of ethanol lignin hydrogenation products

Liquid hydrogenation products of birch ethanol lignin were analyzed by GC-MS (Table 3). The products obtained from the depolymerization of lignin are represented mainly by monomeric methoxyphenols, among which syringol derivatives predominate: syringol, 4-propylsyringol, 4-methylsyringol and, to a lesser extent, guaiacol derivatives.

The use of ruthenium catalysts in the process of hydrogenation of birch ethanol lignin leads to an increase in the total yield of monomers by almost 5 times (Table 2). Moreover, their maximum yield is 11.2 wt% when using a 3%Ru/C (400) catalyst. Among the monomers formed, the predominant one is 4-propylsyringol with a yield of 3.2 wt%. A similar trend was observed during the hydrogenation of birch wood using a Ru/C catalyst (250 °C, 3 h), when the catalyst provided an increase in the yield of methoxyphenols by 4-5 times depending on the processing conditions,¹⁴ and the main monomer was 4-propylsyringol. It should be noted that the yields of methoxyphenols during the hydrogenation of organosolv lignin are lower compared to the hydrogenation of native lignin in the original wood, which is associated with the partial loss of reactive β -O-4 bonds.

It is known from the literature that ruthenium-based catalysts lead to the formation of predominantly propyl-substituted methoxy-

phenols,¹⁵ whereas when using Pd or Ni-containing catalysts, the main content is 4-propanol-substituted methoxyphenols.^{15,16} The results obtained confirm the literature data since the yield of 4-propanosyringol does not exceed 0.3 wt%.

In addition, the acidity of the catalyst also affects the yield of products. Previously, we showed that during the hydrogenation of spruce wood, the highest yield of methoxyphenols was obtained with a Ru/C catalyst having a pH_{pzc} of 7.12,^{9,11} similarly to this work.

Quantum chemical calculations of birch ethanol lignin hydrogenation products

Theoretical methods for studying lignin and its modification products are being actively developed,^{17,18} including calculations of phenyl-propane lignin units,¹⁹ model lignin compounds,²⁰ their derivatives.²¹ For theoretical calculations in such studies, the following models are often used: B3LYP/6-31G*,²⁰ M06/6-31G*,²² M06-2X/6-31+G(d,p),^{23,24} B3LYP/6-311G (d,p),²⁵ *etc.*

The main products of birch ethanol lignin hydrogenation for quantum chemical calculations were: syringol (a), 4-methyl syringol (b), 4-ethyl syringol (c), 4-propyl syringol (d), 4-propenyl syringol (e). The optimized structures of the studied syringol derivatives are presented in Figure 2. According to the data presented in Figure 2 and Table 4, the introduction of an alkyl radical and an increase in its length affects the

interatomic distance in the molecules under study. Thus, the bond lengths in the C1-C2 benzene ring increase from 1.398 to 1.4008 Å when going from syringol to 4-ethyl syringol, then a decrease in this value is observed to 1.3979 and 1.3963 Å for 4-propyl syringol and 4-propenyl syringol, respectively. For the C1-C6 bond, a different picture is observed: a decrease from 1.398 to 1.3936 Å when going from syringol to 4-ethyl syringol, with a subsequent increase to 1.3965 and 1.3952 Å for 4-propyl syringol and 4-propenyl syringol, respectively. For the C2-C3 bond, the following values are observed for substances a-e: 1.3885, 1.3910, 1.3905, 1.3927 and 1.3975 Å. For the C3-C4 bond, the following values are observed for substances a-e: 1.3976, 1.4036, 1.4053, 1.4025 and 1.4084 Å. For the C4-C5 bond for substances a-e the following values are observed: 1.3906, 1.3890, 1.3876, 1.3902, 1.3854 Å. For the C5-C6 bond, the following values are observed for substances a-e: 1.4054, 1.4054, 1.4059, 1.4041 and 1.4077 Å. It should be noted that the C-O bond changes less when an alkyl radical is introduced and increased into the syringol molecule. Thus, the bond lengths in the benzene ring change nonlinearly with the

introduction of an alkyl radical of different lengths.

Mulliken atomic charges

Mulliken atomic charges play an important role in understanding the chemical reactivity of compounds.²⁶⁻³⁰ The calculated and indicated charges of Mulliken atoms for syringol and its derivatives are shown in Table 5. As indicated in Table 5, the C3 atom for 4-propenyl syringol carries the highest positive charge of 1.9733 among the other carbon atoms and is therefore likely to be the site of nucleophilic attack. The C2 atom for 4-ethyl syringol carries the highest negative charge of -1.043 among all syringol derivatives studied. It should be noted that the introduction of an alkyl substituent into the fourth position of syringol affects all Mulliken atomic charges of molecules. At the same time, an increase in the alkyl substituent and the formation of a double carbon-carbon bond does not linearly change the atomic charges. Thus, for the 1C atom for the molecules: syringol, 4-methyl syringol, 4-ethyl syringol, 4-propyl syringol, 4-propenyl syringol, the following values are observed: -0.1919, -0.3893, -0.5138, -0.3868 and 0.0677, respectively.

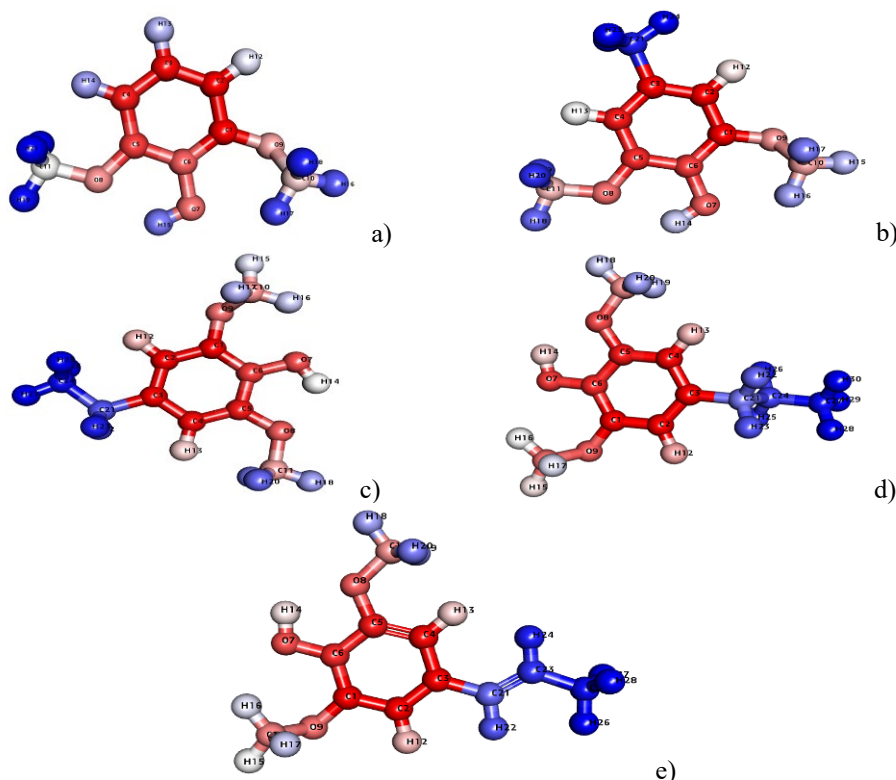


Figure 2: Optimized structure of molecules (a-e)

Table 4
Bond parameters of molecules (a-e)

a		b		c		d		e											
Bond lengths (Å)	Bond angles (°)																		
C1-C2	1.398	C2-C1-C6	119.431	C1-C2	1.3995	C2-C1-C6	119.5705	C1-C2	1.4008	C2-C1-C6	119.7444	C1-C2	1.3979	C2-C1-C6	119.5411	C1-C2	1.3963	C2-C1-C6	119.4433
C1-C6	1.398	C2-C1-O9	118.571	C1-C6	1.3948	C2-C1-O9	118.2063	C1-C6	1.3936	C2-C1-O9	118.0017	C1-C6	1.3965	C2-C1-O9	118.2473	C1-C6	1.3952	C2-C1-O9	118.3681
C1-O9	1.3712	C6-C1-O9	121.8846	C1-O9	1.3718	C6-C1-O9	122.1185	C1-O9	1.3724	C6-C1-O9	122.1456	C1-O9	1.3718	C6-C1-O9	122.1125	C1-O9	1.3715	C6-C1-O9	122.0801
C2-C3	1.3885	C1-C2-C3	120.5383	C2-C3	1.391	C1-C2-C3	121.5962	C2-C3	1.3905	C1-C2-C3	121.5804	C2-C3	1.3927	C1-C2-C3	121.5947	C2-C3	1.3975	C1-C2-C3	121.9477
C2-H12	1.083	C1-C2-H12	117.978	C2-H12	1.0838	C1-C2-H12	117.4566	C2-H12	1.082	C1-C2-H12	116.8422	C2-H12	1.0842	C1-C2-H12	117.4828	C2-H12	1.0838	C1-C2-H12	117.4906
C3-C4	1.3976	C3-C2-H12	121.4819	C3-C4	1.4036	C2-C2-H12	120.9458	C3-C4	1.4053	C2-C2-H12	121.5758	C3-C4	1.4025	C2-C2-H12	120.922	C3-C4	1.4084	C2-C2-H12	120.5596
C3-H13	1.0833	C2-C3-C4	120.566	C3-C21	1.5107	C2-C3-C4	118.7484	C3-C21	1.5202	C2-C3-C4	118.5166	C3-C21	1.513	C2-C3-C4	118.7463	C3-C21	1.4699	C2-C3-C4	118.3134
C4-C5	1.3906	C2-C3-H13	119.9549	C4-C5	1.389	C2-C3-C21	121.1622	C4-C5	1.3876	C2-C3-C21	122.9138	C4-C5	1.3902	C2-C3-C21	120.8553	C4-C5	1.3854	C2-C3-C21	118.7286
C4-H14	1.0816	C4-C3-H13	119.4786	C4-H13	1.0827	C4-C3-C21	120.0887	C4-H13	1.083	C4-C3-C21	118.5685	C4-H13	1.0828	C4-C3-C21	120.3742	C4-H13	1.0808	C4-C3-C21	122.9576
C5-C6	1.4054	C3-C4-C5	118.9855	C5-C6	1.4054	C3-C4-C5	119.9612	C5-C6	1.4059	C3-C4-C5	120.1987	C5-C6	1.4041	C3-C4-C5	119.9872	C5-C6	1.4077	C3-C4-C5	119.9498
C5-O8	1.3753	C3-C4-H14	120.1581	C5-O8	1.3756	C3-C4-H13	119.6091	C5-O8	1.3759	C3-C4-H13	119.4442	C5-O8	1.376	C3-C4-H13	119.5564	C5-O8	1.3752	C3-C4-H13	120.0753
C6-O7	1.3652	C5-C4-H14	120.8561	C6-O7	1.3671	C5-C4-H13	120.4294	C6-O7	1.3672	C5-C4-H13	120.3568	C6-O7	1.3671	C5-C4-H13	120.4564	C6-O7	1.3644	C5-C4-H13	119.9748
O7-H15	0.9671	C4-C5-C6	120.9397	O7-H14	0.9669	C4-C5-C6	121.1374	O7-H14	0.9669	C4-C5-C6	121.0914	O7-H14	0.967	C4-C5-C6	121.089	O7-H14	0.9672	C4-C5-C6	121.3889
O8-C11	1.4226	C5-C5-O8	125.8319	O8-C11	1.4221	C5-C5-O8	125.6854	O8-C11	1.422	C5-C5-O8	125.7375	O8-C11	1.4222	C5-C5-O8	125.6759	O8-C11	1.4226	C5-C5-O8	125.6313
O9-C10	1.4336	C6-C5-O8	113.2221	O9-C10	1.4333	C6-C5-O8	113.171	O9-C10	1.4332	C6-C5-O8	113.1641	O9-C10	1.4335	C6-C5-O8	113.2319	O9-C10	1.4335	C6-C5-O8	112.9746
C10-H16	1.0895	C1-C6-C5	119.5288	C10-H15	1.0896	C1-C6-C5	118.9755	C10-H15	1.0896	C1-C6-C5	118.8575	C10-H15	1.0896	C1-C6-C5	119.0279	C10-H15	1.0895	C1-C6-C5	118.9467
C10-H17	1.0912	C1-C6-O7	120.4469	C10-H16	1.0911	C1-C6-O7	120.835	C10-H16	1.0911	C1-C6-O7	120.9632	C10-H16	1.091	C1-C6-O7	120.7807	C10-H16	1.0912	C1-C6-O7	120.8768
C10-H18	1.0957	C5-C6-O7	120.0193	C10-H17	1.0958	C5-C6-O7	120.1836	C10-H17	1.0958	C5-C6-O7	120.1726	C10-H17	1.0957	C5-C6-O7	120.1889	C10-H17	1.0957	C5-C6-O7	120.1713
C11-H19	1.0887	C6-O7-H15	107.3172	C11-H18	1.0887	C6-O7-H14	107.2411	C11-H18	1.0888	C6-O7-H14	107.2183	C11-H18	1.0887	C6-O7-H14	107.2123	C11-H18	1.0887	C6-O7-H14	107.2829
C11-H20	1.0946	C5-O8-C11	118.5555	C11-H19	1.0947	C5-O8-C11	118.6525	C11-H19	1.0947	C5-O8-C11	118.6297	C11-H19	1.0947	C5-O8-C11	118.6205	C11-H19	1.0946	C5-O8-C11	118.6717
C11-H21	1.0946	C1-O9-C10	116.7102	C11-H20	1.0947	C1-O9-C10	116.7258	C11-H20	1.0948	C1-O9-C10	116.7763	C11-H20	1.0947	C1-O9-C10	116.8174	C11-H20	1.0947	C1-O9-C10	116.6658
		O9-C10-H16	105.8295	C21-H22	1.0948	O9-C10-H15	105.831	C21-H22	1.0968	O9-C10-H15	105.8319	C21-H22	1.0963	O9-C10-H15	105.8196	C21-H22	1.0889	O9-C10-H15	105.8277
		O9-C10-H17	111.4631	C21-H23	1.0948	O9-C10-H16	111.4782	C21-H23	1.097	O9-C10-H16	111.4983	C21-H23	1.0955	O9-C10-H16	111.4836	C21-C23	1.3388	O9-C10-H16	111.48
		O9-C10-H18	110.3397	C21-H24	1.0915	O9-C10-H17	110.3421	C21-C24	1.5296	O9-C10-H17	110.358	C21-C24	1.5411	O9-C10-H17	110.3548	C23-H24	1.0883	O9-C10-H17	110.3459

H16- C10- H17	109.8136	H15- C10- H16	109.8484	C24- H25	1.0934	H15- C10- H16	109.8473	C24- H25	1.0954	H15- C10- H16	109.8521	C23- C25	1.4994	H15- C10- H16	109.8054
H16- C10- H18	109.39	H15- C10- H17	109385	C24- H26	1.0934	H15- C10- H17	109.3757	C24- H26	1.0958	H15- C10- H17	109.374	C25- H26	1.0927	H15- C10- H17	109.3944
H17- C10- H18	109.9152	H16- C10- H17	109.8687	C24- H27	1.093	H16- C10- H17	109.8428	C24- C27	1.531	H16- C10- H17	109.8687	C25- H27	1.0963	H16- C10- H17	109.8983
O8- C11- H19	106.0291	O8- C11- H18	106.028			O8- C11- H18	106.0356	C27- H28	1.0946	O8- C11- H18	106.0304	C25- H28	1.0963	O8- C11- H18	106.0102
O8- C11- H20	111.0543	O8- C11- H19	111.0988			O8- C11- H19	111.1003	C27- H29	1.0935	O8- C11- H19	111.0725			O8- C11- H19	111.0591
O8- C11- H21	111.0745	O8- C11- H20	111.0888			O8- C11- H20	111.0976	C27- H30	1.0948	O8- C11- H20	111.1272			O8- C11- H20	111.0735
H19- C11- H20	109.524	H18- C11- H19	109.5021			H18- C11- H19	109.4986			H18- C11- H19	109.5169			H18- C11- H19	109.5268
H19- C11- H21	109.4542	H18- C11- H20	109.4454			H18- C11- H20	109.4438			H18- C11- H20	109.4245			H18- C11- H20	109.4527
H20- C11- H21	109.6304	H19- C11- H20	109.6033			H19- C11- H20	109.591			H19- C11- H20	109.595			H19- C11- H20	109.6432
		C3- C21- H22	111.3706			C3- C21- H22	108.3071			C3- C21- H22	109.614			C3- C21- H22	114.297
		C3- C21- H23	111.4222			C3- C21- H23	108.4221			C3- C21- H23	109.3901			C3- C21- H23	128.0423
		C3- C21- H24	111.1213			C3- C21- H24	116.3648			C3- C21- H24	113.382			H22- C21- H23	117.6606
		H22- C21- H23	107.2775			H22- C21- H23	105.4876			H22- C21- H23	106.3403			C21- C23- H24	119.7526
		H22- C21- H24	107.7076			H22- C21- H24	108.8524			H22- C21- H24	108.951			C21- C23- C25	124.5942
		H23- C21- H24	107.7467			H23- C21- H24	108.8668			H23- C21- H24	108.9196			H24- C23- C25	115.6531
						C21- C24- H25	111.7215			C21- C24- H25	108.8996			C23- C25- H26	111.5417
						C21- C24- H26	111.6558			C21- C24- H26	109.0345			C23- C25- H27	111.2486
						C21- C24- H27	110.1673			C21- C24- H27	112.9311			C23- C25- H28	111.25
						H25- C24- H26	107.9087			H25- C24- H26	106.0813			H26- C25- H27	108.0321
						H25- C24- H27	107.5573			H25- C24- H27	109.8509			H26- C25- H28	108.0286
						H26- C24- H27	107.6481			H26- C24- H27	109.8071			H27- C25- H28	106.5265
										C24- C27- H28	111.2402				
										C24- C27- H29	111.2757				
										C24- C27- H30	111.3052				
										H28-	107.6355				

	C27- H29
	H28- C27- 107.5373 H30
	H29- C27- 107.6576 H30

Table 5
Mulliken atomic charges of molecules (a-e)

a		b		c		d		e	
Atoms	Charges								
1C	-0.1919	1C	-0.3893	1C	-0.5138	1C	-0.3868	1C	0.0677
2C	0.2984	2C	-0.6428	2C	-1.0430	2C	-0.2394	2C	-0.2067
3C	-0.2856	3C	0.5481	3C	1.4826	3C	1.5999	3C	1.9733
4C	0.2367	4C	0.4197	4C	0.3070	4C	0.0494	4C	-0.9458
5C	0.0280	5C	-0.1419	5C	-0.5114	5C	-0.3938	5C	-0.5962
6C	-0.5266	6C	-0.0848	6C	0.1316	6C	-0.3407	6C	-0.3005
7O	-0.2762	7O	-0.2838	7O	-0.2876	7O	-0.2786	7O	-0.2760
8O	-0.2665	8O	-0.2634	8O	-0.2599	8O	-0.2635	8O	-0.2694
9O	-0.1738	9O	-0.1647	9O	-0.1556	9O	-0.1732	9O	-0.1673
10C	-0.2810	10C	-0.2922	10C	-0.2996	10C	-0.3038	10C	-0.2971
11C	-0.2945	11C	-0.2951	11C	-0.3361	11C	-0.3349	11C	-0.3111
12H	0.1806	12H	0.1549	12H	0.1773	12H	0.2016	12H	0.1697
13H	0.1698	13H	0.1403	13H	0.1514	13H	0.1735	13H	-0.0510
14H	0.1472	14H	0.3014	14H	0.3047	14H	0.2997	14H	0.3029
15H	0.3012	15H	0.1495	15H	0.1488	15H	0.1505	15H	0.1499
16H	0.1510	16H	0.1636	16H	0.1651	16H	0.1664	16H	0.1638
17H	0.1630	17H	0.1265	17H	0.1275	17H	0.1261	17H	0.1297
18H	0.1244	18H	0.1799	18H	0.1679	18H	0.1701	18H	0.1818
19H	0.1698	19H	0.1657	19H	0.1660	19H	0.1665	19H	0.1699
20H	0.1648	20H	0.1626	20H	0.1619	20H	0.1628	20H	0.1664
21H	0.1612	21C	-0.4214	21C	-0.2986	21C	-0.7247	21C	0.1290
		22H	0.1578	22H	0.1537	22H	0.1327	22H	0.1012
		23H	0.1543	23H	0.1556	23H	0.1537	23C	-0.2724
		24H	0.1550	24C	-0.5498	24C	-0.1597	24H	0.1319
				25H	0.1466	25H	0.1462	25C	-0.5765
				26H	0.1499	26H	0.1306	26H	0.1433
				27H	0.1580	27C	-0.6363	27H	0.1447
						28H	0.1304	28H	0.1447
						29H	0.1468		
						30H	0.1282		

For the 2C atom in the molecules of syringol derivatives, with increasing length and nature of the alkyl substituent, the Mulliken atomic charges values are observed: 0.2984, -0.6428, -1.0430, -0.2394 and -0.2067, respectively. For the 3C atom in the series syringol, 4-methyl syringol, 4-ethyl syringol, 4-propyl syringol, 4-propenyl syringol, the following values are observed: -0.2856, 0.5481, 1.4826, 1.5999 and 1.9733, respectively. In general, a similar picture is observed for other atoms, carbon, oxygen and hydrogen.

HOMO-LUMO

Frontier molecular orbitals, namely HOMO and LUMO, play an important role in quantum chemistry. Lowest unoccupied molecular orbitals (LUMO) and highest occupied molecular orbitals (HOMO), and their properties are very useful for materials scientists, physicists and chemists.³¹ The energy separation of the highest occupied molecular orbital (HOMO) and lowest unoccupied molecular orbital (LUMO) has been used as a simple indicator of kinetic stability.^{32,33}

A large HOMO-LUMO gap implies high kinetic stability and low chemical reactivity, since it is energetically unfavorable to add electrons to a high-lying LUMO, extract electrons from a low-lying HOMO, and thus form an activated complex of any reaction potential.³⁴ Pearson noted that the HOMO-LUMO gap reflects the chemical stability of the molecule.^{35,36} In general, an atom with a

higher density HOMO should have a higher ability to remove an electron, while an atom with a higher density occupied by a LUMO should have a higher force to gain an electron.³⁷⁻³⁹ Blue and red colors represent positive and negative phases, respectively. Data from the HOMO-LUMO analysis are presented in Figure 3 and Table 6.

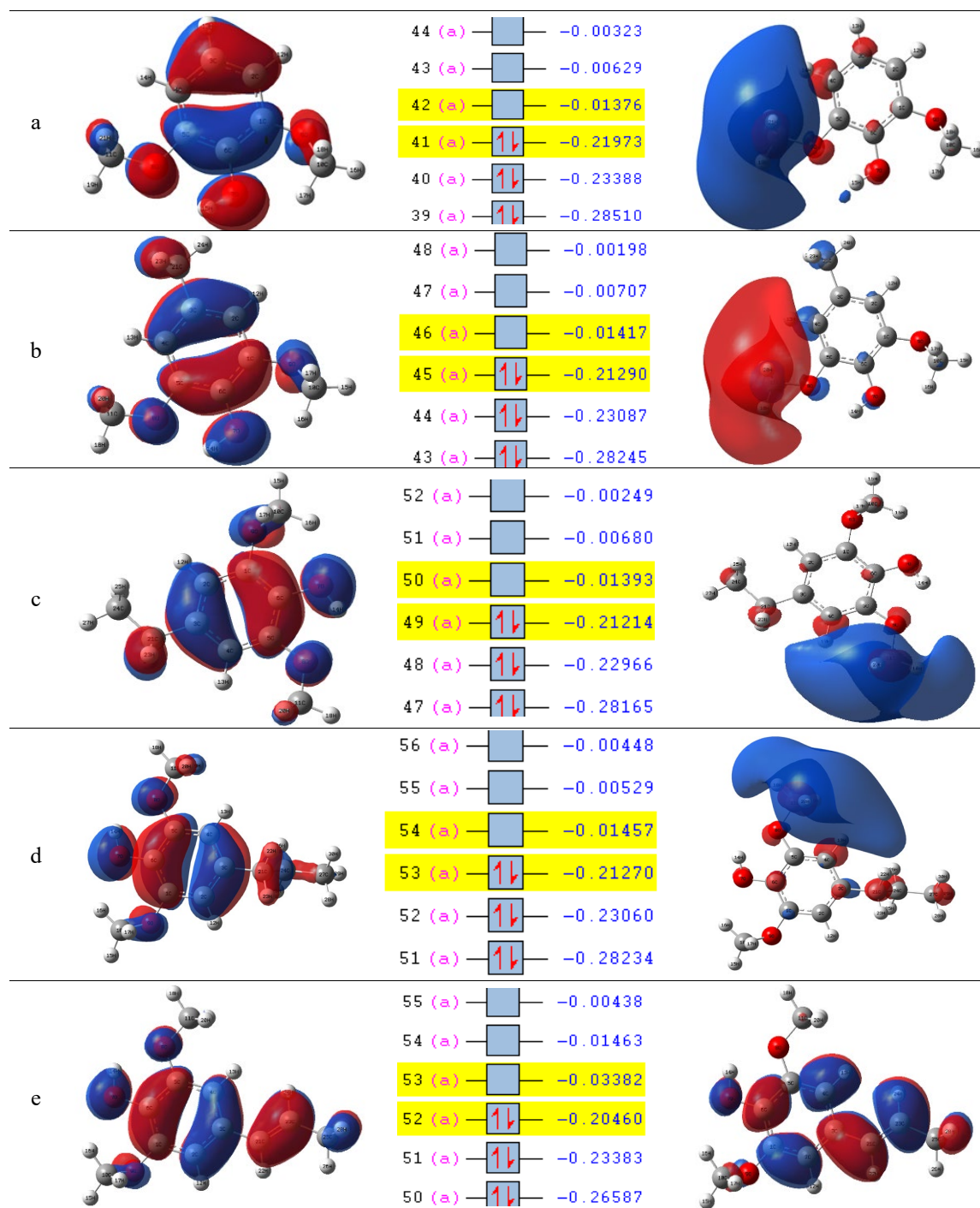


Figure 3: HOMO-LUMO orbitals and energy ranges of molecules (a-e)

Table 6
Calculated electronic parameters of molecules (a-e) using B3LYP/6-311++G(d,p)

	a	b	c	d	e
E_{LUMO}	-0.3744	-0.3856	-0.3791	-0.3965	-0.9203
E_{HOMO}	-5.9792	-5.7933	-5.7726	-5.7879	-5.5675
Energy band gap (ΔE)	5.6047	5.4077	5.3936	5.3914	4.6472
Electronegativity (χ)	3.1768	3.0894	3.0758	3.0922	3.2439
Electrophilicity index (ω)	1.8006	1.7650	1.7541	1.7735	2.2643
Chemical potential (μ)	-3.1768	-3.0894	-3.0758	-3.0922	-3.2439
Chemical hardness (η)	2.8024	2.7039	2.6968	2.6957	2.3236
Optical softness (σ_s)	0.1784	0.1849	0.1854	0.1855	0.2152
Softness (ζ)	0.3568	0.3698	0.3708	0.3710	0.4304
Ionization energy (IP)	5.9792	5.7933	5.7726	5.7879	5.5675
Maximum charge transfer index (ΔN_{max})	1.1336	1.1426	1.1406	1.1471	1.3961
Nucleophilic index (N)	0.5554	0.5666	0.5701	0.5639	0.4416
Electron affinity (EA)	0.3744	0.3856	0.3791	0.3965	0.9203

According to the data presented in Table 6, the LUMO energy gradually decreases with increasing length of the alkyl radical, and decreases significantly when moving from the propyl radical to the propenyl radical, which is due to the influence of the double bond on the overall energy structure. In turn, the energy of HOMO does not change linearly. It should be noted that when going from syringol to 4-methylsyringol and from 4-propyl syringol to 4-propenyl syringol, the largest change in HOMO energy values is observed. The Energy Band Gap gradually decreases with increasing length of the alkyl radical. The greatest change is observed when moving from 4-propyl syringol to 4-propenyl syringol, which is associated with an increase in its chemical activity due to the presence of a double bond.

The introduction of an alkyl radical reduces the electronegativity and electrophilicity index of syringol, and the presence of a double bond in the alkyl radical increases the value of this parameter. The values of chemical hardness and ionization energy naturally decrease with the increase in the chain of the alkyl radical; the presence of a double bond for these parameters also leads to their decrease. The optical softness, softness and maximum charge transfer index values increase with increasing chain length of the alkyl radical and the appearance of a double bond. The

nucleophilic index and electron affinity values change nonlinearly with changes in the length of the alkyl substituent in syringol derivatives.

MEP and ALIE analysis

MEP-ALIE analysis is a promising tool in quantum chemistry for identifying effects in atoms and their interactions.⁴⁰ Average local ionization energy (ALIE) is defined as the energy required to remove an electron from a specific region of a molecule.^{41,42} At the same time, to assess molecular regions prone to electrophilic or nucleophilic attacks, the molecular electrostatic potential (MEP) is most often used.⁴³ The MEP is well visualized when its values are compared to the electron density surface. MEP and ALIE complement each other well, since MEP is often used to determine regions of molecules prone to electrophilic attack, and ALIE provides information on the amount of energy required to remove an electron from a molecule.^{44,45}

According to Figure 4, the ALIE surface for the test substances is colored blue over the benzene ring and red over the alkyl and methoxy groups; for 4-propenic syringol, blue is also found over the carbon-carbon double bond. On MEP maps, the surface above the methoxy groups is light blue, the alkyl substituent is blue-green, and the benzene ring is yellow.

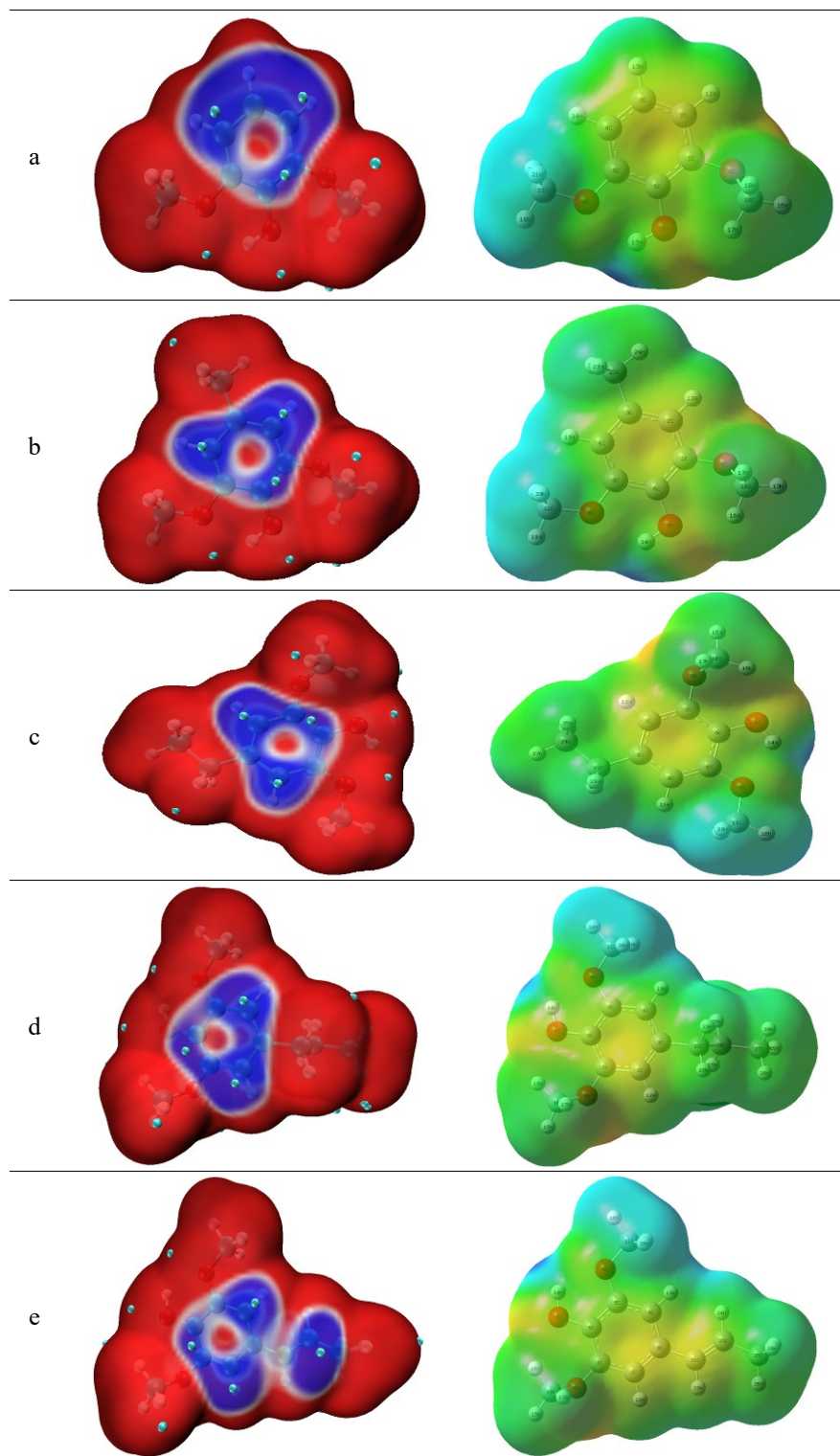


Figure 4: ALIE (average local ionization energy) and MEP (molecular electrostatic potential) surfaces of molecules (a-e)

Spectroscopic analysis of birch ethanol lignin hydrogenation products

Lignin and its modification products are actively studied by experimental and theoretical spectroscopic methods.⁴⁶⁻⁴⁸ The theoretical spectra

of the studied syringol derivatives are presented in Figure 5, and the corresponding absorption bands for the bonds are presented in Table 7.

OH group

The hydroxyl group for syringol and its derivatives is identified in the FTIR spectra in the region of 3700-3600 cm^{-1} .⁴⁹ In all the presented spectra, it has a clear absorption band of noticeable intensity, without splitting into other bands.

C-O group

The C-O group in theoretical FTIR spectra is observed in the regions of 1470-1530, 1210-1310, 1070-1120 and 1000-1090 cm^{-1} . Vibrations of this group are widespread and have been actively studied in previous works.^{50,51}

C-C group

The study of carbon-carbon bonds in biomass components and products of its processing by

spectroscopic methods is actively being studied.^{52,53} In our case, when studying syringol and its derivatives, vibrations of the carbon-carbon bond are observed in the regions: 1440-1600 cm^{-1} (for the aromatic ring), 1640-1670 cm^{-1} (for the double bond in 4-propenyl syringol).

C-H group

Vibrations of the C-H group in theoretical FTIR spectra for the substances under study are observed in the region of 2900-3200 cm^{-1} . In this region, many peaks of varying intensity are observed, which is due to the presence of many C-H bonds in the molecules of syringol and its derivatives. Vibrations of this group were also studied in previous reports.^{54,55}

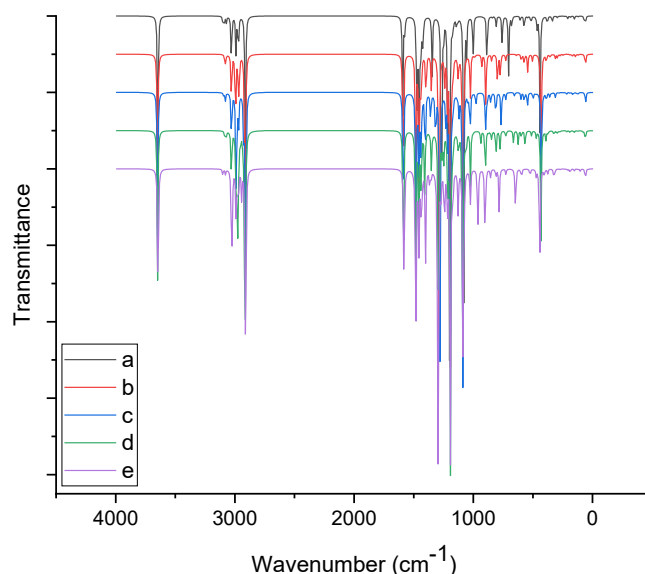
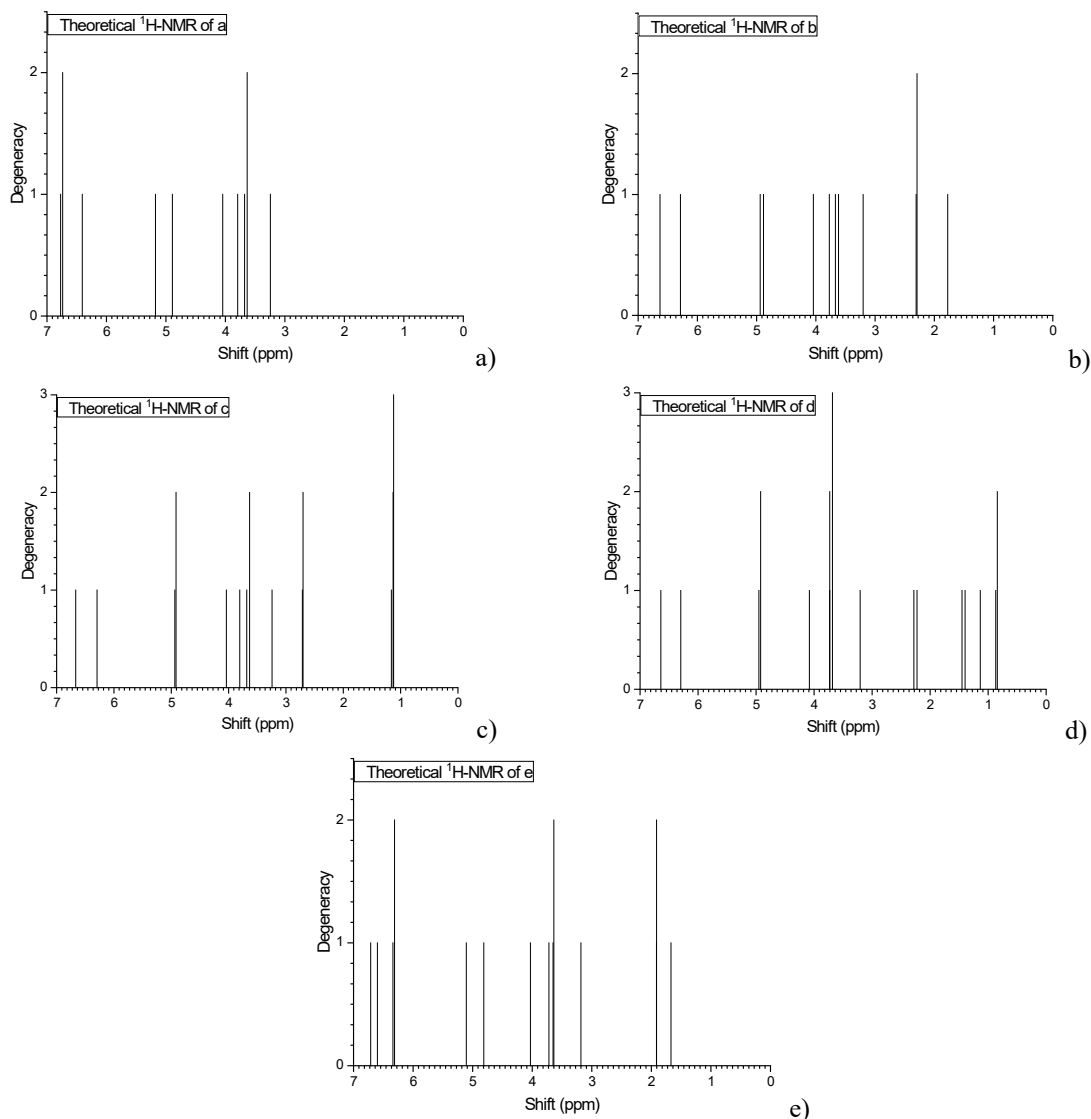


Figure 5: FTIR spectra of molecules (a-e)

Table 7
Calculated vibrational frequency (B3LYP/6-311G++(d,p) with PED assignments with VEDA 4 of a (scaled by 0.9668)

No	Theoretical wavenumber (cm^{-1})			PED (%) Assignments
	Unscaled	Scaled	IR intensity	
1	3771.23	3646.025164	114.56	v OH (100)
2	3207.63	3101.136684	5.45	v CH (14)+v CH (80)
3	3197.33	3091.178644	7.27	v CH (77)+v CH (10)+v CH (-13)
4	3178.43	3072.906124	5.25	v CH (-18)+v CH (76)
5	3136.46	3032.329528	18.60	v CH (90)
6	3131.78	3027.804904	19.57	v CH (74)+v CH (-25)
7	3093.99	2991.269532	29.58	v CH (16)+v CH (59)+v CH (-25)
8	3073.6	2971.55648	32.27	v CH (-50)+v CH (50)
9	3013.59	2913.538812	58.76	v CH (10)+v CH (15)+v CH (72)

10	3012.31	2912.301308	64.99	v CH (-44)+v CH (-44)
11	1647.44	1592.744992	77.09	v CC (30)+v CC (-23)+ δ CCC (11)
12	1628.59	1574.520812	13.37	v CC (34)+v CC (10)+v CC (-12)
13	1524.93	1474.302324	85.64	v OC (-10)+ δ HCC (11)
14	1511.22	1461.047496	11.93	δ HCH (-18)+ δ HCH (52)+ τ HCOC (12)
15	1508.04	1457.973072	32.66	δ HCC (-16)+ δ HCH (11)+ δ HCH (-23)+
16	1503.75	1453.8255	92.42	δ HCH (-15)+ δ HCH (-14)+ δ HCH (35)+
17	1489.68	1440.222624	9.76	δ HCH (-38)+ δ HCH (35)+ τ HCOC (19)
18	1486.94	1437.573592	17.24	δ HCH (-41)+ δ HCH (26)+ τ HCOC (13)
19	1475.51	1426.523068	18.94	δ HCH (23)+ δ HCH (27)+ δ HCH (15)
20	1469.04	1420.267872	13.28	δ HCH (27)+ δ HCH (20)+ δ HCH (15)
21	1391.21	1345.021828	47.79	v CC (-17)+ δ HOC (29)+ δ HCC (11)
22	1311.38	1267.842184	208.24	v OC (-10)+v OC (-13)+ δ HOC (18)+v CH ()
23	1291.95	1249.05726	12.40	v CC (25)+ δ HCC (-13)
24	1257.29	1215.547972	88.54	v OC (-24)+v OC (21)+ δ CCC (12)+ δ HCC (10)
25	1241.46	1200.243528	255.33	v CC (-11)+v OC (-13)+v OC (20)+ δ HOC (12)
26	1213.24	1172.960432	11.80	δ HCH (12)+ τ HCOC (19)+ τ HCOC (-25)
27	1201.45	1161.56186	0.82	δ HCH (11)+ τ HCOC (21)+ τ HCOC (-22)
28	1181.31	1142.090508	6.24	δ HCC (-18)+ δ HCC (35)+ δ HCC (-13)
29	1170.89	1132.016452	3.13	δ HCH (13)+ δ HCH (-16)+ τ HCOC (-32)+ τ HCOC (23)+ τ HCOC(15)
30	1169.94	1131.097992	0.63	δ HCH (-13)+ δ HCH (13)+ τ HCOC (39)+ τ HCOC (-17)+ τ HCOC (-17)
31	1116.87	1079.789916	216.65	v OC (43)
32	1092.9	1056.61572	27.73	v CC (21)+v CC (19)+ δ HCC (26)
33	1036.51	1002.097868	36.16	v OC (12)+v OC (65)
34	948.13	916.652084	0.82	τ HCCC (-35)+ τ HCCC (45)
35	915.61	885.211748	44.73	v OC (-17)+v OC (16)+v OC (19)+v OC (-14)
36	869.72	840.845296	1.03	τ HCCC (30)+ τ HCCC (10)+ τ HCCC (41)
37	836.91	809.124588	8.32	v OC (22)+ δ CCC (-14)+ δ CCC (32)
38	784.11	758.077548	24.43	τ HCCC (-16)+ τ HCCC (10)+OUT OCCC (-13)+ OUT OCCC (15)+OUT OCCC (16)
39	728.8	704.60384	46.15	τ HCCC (21)+ τ HCCC (16)+ τ HCCC (-26)+OUT OCCC (-13)
40	701.04	677.765472	8.27	v CC (12)+v OC (11)+ δ CCC (10)
41	626.88	606.067584	3.59	δ COC (-14)+OUT OCCC (-31)+OUT OCCC 21)
42	592.83	573.148044	10.82	δ OCC (25)+ δ OCC (12)
43	561.51	542.867868	1.01	τ CCCC (36)+ τ CCCC (-16)+ τ CCCC (11)+OUT OCCC (20)
44	533.57	515.855476	6.12	δ CCC (-13)+ δ CCC (22)+ δ CCC (-10)+ δ CCC (10)
45	480.91	464.943788	9.28	v OC (-10)+ δ CCC (22)+ δ CCC (-13)+ δ OCC (-10)
46	455.3	440.18404	88.19	τ HOCC (93)
47	393.19	380.136092	6.80	δ OCC (14)+ δ COC (-18)+ δ COC (20)
48	350.07	338.447676	5.12	δ OCC (-19)+ δ COC (14)+ δ COC (11)+OUT OCCC (-13)
49	305.26	295.125368	1.20	δ OCC (-30)+ δ OCC (17)+OUT OCCC (12)
50	284.36	274.919248	0.35	τ CCCC (14)
51	243.75	235.6575	0.33	δ OCC (11)+ δ COC (-14)+ τ CCCC (-13)
52	216.56	209.370208	2.21	δ OCC (22)+ δ COC (-15)+ τ HCOC (-12)
53	192.87	186.466716	1.25	τ HCOC (10)+ τ CCCC (17)+ τ CCCC (-12)
54	157.84	152.599712	2.35	τ HCOC (35)+ τ HCOC (10)+ τ CCCC (-10)
55	125.59	121.420412	0.58	τ CCCC (-12)+ τ CCCC (11)+ τ CCCC (26)+ τ COCC(14)+OUT OCCC (-13)
56	71.21	68.845828	3.35	τ COCC (-63)
57	60.98	58.955464	5.69	τ COCC (66)

Figure 6: $^1\text{H-NMR}$ spectra of molecules (a-e)

NMR spectroscopy has proven itself well as an analysis of biomass processing products.^{24,56,57} Syringol and its derivatives are products of various catalytic processes for processing various types of biomass.⁵⁸ Determination of syringol derivatives by NMR spectroscopy is important for their identification and subsequent regulation of experimental conditions.⁵⁹ Calculation of the NMR spectra of syringol and its alkyl derivatives can make it possible to determine them in more detail in the products of various thermocatalytic processes of biomass processing. The calculated NMR spectra are shown in Figure 6, and their corresponding values are shown in Table 8.

According to the data presented in Table 8, the introduction of an alkyl substituent leads to a change (shift and/or change in intensity) of most

chemical shifts in the spectra of syringol derivatives. Thus, the 12-H value for the original syringol is 6.7709 ppm, for 4-methyl syringol – 6.6304 ppm, for 4-ethyl syringol – 6.6671 ppm, for 4-propyl syringol – 6.6412 ppm, and for 4-propenyl syringol – 6.713 ppm. For the 13-H atom in the series: syringol, 4-methyl syringol, 4-ethyl syringol, 4-propyl syringol, 4-propenyl syringol, the following values are observed: 6.7369, 6.2861, 6.2953, 6.2983 and 6.5997 ppm, respectively. For the 14-H atom in the molecules of syringol derivatives, with increasing length and nature of the alkyl substituent, the following values are observed: 6.4067, 4.9392, 4.9179, 4.922 and 5.1072 ppm, respectively. For other hydrogen atoms, changes in the NMR spectra are also observed, as shown in Figure 6 and Table 8.

Table 8
Chemical shifts of hydrogen atoms for molecules (a-e)

a		b		c		d		e	
12-H	6.7709	12-H	6.6304	12-H	6.6671	12-H	6.6412	13-H	6.713
13-H	6.7369	13-H	6.2861	13-H	6.2953	13-H	6.2983	12-H	6.5997
14-H	6.4067	14-H	4.9392	16-H	4.9383	16-H	4.9513	24-H	6.3389
15-H	5.1768	16-H	4.8835	14-H	4.9179	14-H	4.922	22-H	6.311
17-H	4.8915	18-H	4.0428	18-H	4.0392	18-H	4.0814	14-H	5.1072
19-H	4.0451	15-H	3.7721	15-H	3.8058	15-H	3.7309	16-H	4.8131
16-H	3.7931	20-H	3.6704	20-H	3.6833	20-H	3.7297	18-H	4.0297
21-H	3.6779	19-H	3.6172	19-H	3.6339	19-H	3.683	15-H	3.72
20-H	3.6339	17-H	3.2011	17-H	3.2421	17-H	3.2064	19-H	3.6511
18-H	3.2446	22-H	2.3065	23-H	2.7142	23-H	2.2806	20-H	3.6366
12-H	6.7709	23-H	2.2921	22-H	2.7011	22-H	2.2259	17-H	3.1819
13-H	6.7369	24-H	1.7738	25-H	1.161	25-H	1.4503	27-H	1.9136
14-H	6.4067			27-H	1.1303	26-H	1.398	28-H	1.9134
15-H	5.1768			26-H	1.1216	29-H	1.1361	26-H	1.6699
						28-H	0.8687		
						30-H	0.8419		

CONCLUSION

The effect of solid bifunctional ruthenium-containing catalysts on the yield and composition of birch ethanol lignin hydrogenation products has been established. It has been shown that the most effective catalyst is 3% Ru/C with a support oxidation temperature of 400 °C. The use of this catalyst ensures the maximum production of monomeric methoxyphenols with a yield of about 11.1 wt%. The main components of the liquid products are alkyl derivatives of syringol. The main derivatives of 4-alkylsyringol have been studied using the density functional theory method. Spectroscopic (FTIR and NMR) characteristics, HOMO-LUMO, Mulliken atomic charges, electronic parameters, MEP and ALIE have been calculated for these molecules. The effect of the length and nature of the alkyl (or allyl) radical on the energy structure and physicochemical parameters of the syringol derivative has been shown. The introduction of an alkyl radical reduces the electronegativity and electrophilicity index of syringol, and the presence of a double bond in the alkyl radical increases the value of this parameter. The values of chemical hardness and ionization energy naturally decrease with the increase in the chain of the alkyl radical; the presence of a double bond for these parameters also leads to their decrease. The results obtained may subsequently help in the identification of syringol derivatives in multicomponent mixtures, such as wood hydrogenation products and hardwood lignin.

ACKNOWLEDGEMENTS: The authors would like to thank Bitlis Eren University for Gaussian software and Bingöl University for the server. Experimental work was conducted within the framework of the budget plan # 0287-2021-0012 for Institute of Chemistry and Chemical Technology SB RAS using the equipment of Krasnoyarsk Regional Research Equipment Center of SB RAS.

REFERENCES

- J. S. Luterbacher, D. Martin Alonso and J. A. Dumesic, *Green Chem.*, **16**, 4816 (2014), <https://doi.org/10.1039/c4gc01160k>
- W. Schutyser, T. Renders, S. Van den Bosch, S. F. Koelewijn, G. T. Beckham *et al.*, *Chem. Soc. Rev.*, **47**, 852 (2018), <https://doi.org/10.1039/c7cs00566k>
- K. Zhang, Z. Pei and D. Wang, *Bioresour. Technol.*, **199**, 21 (2016), <https://doi.org/10.1016/j.biortech.2015.08.102>
- A. R. Mankar, A. Pandey, A. Modak and K. K. Pant, *Bioresour. Technol.*, **334**, 125235 (2021), <https://doi.org/10.1016/j.biortech.2021.125235>
- K. Tekin, N. Hao, S. Karagoz and A. J. Ragauskas, *ChemSusChem*, **11**, 3559 (2018), <https://doi.org/10.1002/cssc.201801291>
- J.-Y. Kim, J. Park, H. Hwang, J. K. Kim, I. K. Song *et al.*, *J. Anal. Appl. Pyrol.*, **113**, 99 (2015), <https://doi.org/10.1016/j.jaap.2014.11.011>
- J.-Y. Kim, J. Park, U.-J. Kim and J. W. Choi, *Energ. Fuels*, **29**, 5154 (2015), <https://doi.org/10.1021/acs.energyfuels.5b01055>
- A. S. Kazachenko, V. E. Tarabanko, A. V. Miroshnikova, V. V. Sychev, A. M. Skripnikov *et al.*, *Catalysts*, **11**, 970 (2021), <https://doi.org/10.3390/catal11080970>

- ⁹ O. P. Taran, A. V. Miroshnikova, S. V. Baryshnikov, A. S. Kazachenko, A. M. Skripnikov *et al.*, *Catalysts*, **12**, 1384 (2022), <https://doi.org/10.3390/catal12111384>
- ¹⁰ J. Quesada-Medina, F. J. López-Cremades and P. Olivares-Carrillo, *Bioresour. Technol.*, **101**, 8252 (2010), <https://doi.org/10.1016/j.biortech.2010.06.011>
- ¹¹ O. P. Taran, E. M. Polyanskaya, O. L. Ogorodnikova, C. Descorme, M. Besson *et al.*, *Catal. Ind.*, **2**, 381 (2010), <https://doi.org/10.1134/s2070050410040136>
- ¹² M. J. Frisch, G. W. Trucks, H. B. Schlegel, G. E. Scuseria, M. A. Robb *et al.*, Gaussian, Inc., Wallingford CT, 2009
- ¹³ Gaussian, Inc., Semichem. Inc., 2000-2003, Pittsburgh PA
- ¹⁴ B. N. Kuznetsov, S. V. Baryshnikov, A. V. Miroshnikova, A. S. Kazachenko, Y. N. Malyar *et al.*, *Catalysts*, **11**, 1362 (2021), <https://doi.org/10.3390/catal11111362>
- ¹⁵ S. Van den Bosch, W. Schutyser, S. F. Koelewijn, T. Renders, C. M. Courtin *et al.*, *Chem. Commun.*, **51**, 13158 (2015), <https://doi.org/10.1039/c5cc04025f>
- ¹⁶ Y. Zhai, C. Li, G. Xu, Y. Ma, X. Liu *et al.*, *Green Chem.*, **19**, 1895 (2017), <https://doi.org/10.1039/C7GC00149E>
- ¹⁷ L. Lauberte, G. Fabre, J. Ponomarenko, T. Dizhbite, D. V. Evtuguin *et al.*, *Molecules*, **24**, 1794 (2019), <https://doi.org/10.3390/molecules24091794>
- ¹⁸ A. S. Kazachenko, F. Akman, N. Y. Vasilieva, Y. N. Malyar, O. Y. Fetisova *et al.*, *Polymers*, **14**, 3000 (2022), <https://doi.org/10.3390/polym14153000>
- ¹⁹ F. Akman, *Cellulose Chem. Technol.*, **53**, 243 (2019), <https://doi.org/10.35812/CelluloseChemTechnol.2019.53.24>
- ²⁰ F. Mostaghni, A. Teimouri and S. A. Mirshokraei, *Spectrochim. Acta A: Mol. Biomol. Spectrosc.*, **110**, 430 (2013), <https://doi.org/10.1016/j.saa.2013.03.075>
- ²¹ F. Akman, A. Kazachenko and Y. Malyar, *Cellulose Chem. Technol.*, **55**, 41 (2021), <https://doi.org/10.35812/CelluloseChemTechnol.2021.55.05>
- ²² M. Mensah, R. Tia, E. Adei and N. H. de Leeuw, *Frontiers Chem.*, **10** (2022), <https://doi.org/10.3389/fchem.2022.793759>
- ²³ Z. Wang, M. Hao, X. Li, B. Zhang, M. Jiao *et al.*, *iScience*, **25**, 103755 (2022), <https://doi.org/10.1016/j.isci.2022.103755>
- ²⁴ M. Karlsson, J. Romson, T. Elder, Å. Emmer and M. Lawoko, *Biomacromolecules*, **24**, 1834 (2023), <https://doi.org/10.1021/acs.biomac.3c00186>
- ²⁵ C. Zhu, J.-P. Cao, X.-B. Feng, X.-Y. Zhao, Z. Yang *et al.*, *Renew. Energ.*, **163**, 1831 (2021), <https://doi.org/10.1016/j.renene.2020.10.094>
- ²⁶ R. S. Mulliken, *J. Chem. Phys.*, **7**, 20 (1939), <https://doi.org/10.1063/1.1750319>
- ²⁷ R. S. Mulliken, *Phys. Rev.*, **32**, 186 (1928), <https://doi.org/10.1103/PhysRev.32.186>
- ²⁸ R. S. Mulliken, *Phys. Rev.*, **41**, 49 (1932), <https://doi.org/10.1103/PhysRev.41.49>
- ²⁹ S. C. North, K. R. Jorgensen, J. Pricetolstoy and A. K. Wilson, *Frontiers Chem.*, **11** (2023), <https://doi.org/10.3389/fchem.2023.1152500>
- ³⁰ K. B. Wiberg and P. R. Rablen, *J. Org. Chem.*, **83**, 15463 (2018), <https://doi.org/10.1021/acs.joc.8b02740>
- ³¹ R. G. Parr and W. Yang, "Density Functional Theory of Atoms and Molecules", Oxford University Press, Oxford, 1989
- ³² J.-I. Aihara, *J. Phys. Chem. A*, **103**, 7487 (1999), <https://doi.org/10.1021/jp990092i>
- ³³ N. Nehra, R. K. Tittal and V. D. Ghule, *ACS Omega*, **6**, 27089 (2021), <https://doi.org/10.1021/acsomega.1c03668>
- ³⁴ U. Hashmat, N. Rasool, S. Kausar, A. A. Altaf, S. Sultana *et al.*, *ACS Omega*, **9**, 13917 (2024), <https://doi.org/10.1021/acsomega.3c09182>
- ³⁵ S. Aslam, M. Haroon, T. Akhtar, M. Arshad, M. Khalid *et al.*, *ACS Omega*, **7**, 31036 (2022), <https://doi.org/10.1021/acsomega.2c02805>
- ³⁶ A. S. Kazachenko, F. Akman, N. Y. Vasilieva, N. Issaoui, Y. N. Malyar *et al.*, *Int. J. Mol. Sci.*, **23**, 1602 (2022), <https://doi.org/10.3390/ijms23031602>
- ³⁷ P. S. Kumar, K. Vasudevan, A. Prakasam, M. Geetha and P. M. Anbarasan, *Spectrochim. Acta A: Mol. Biomol. Spectrosc.*, **77**, 45 (2010), <https://doi.org/10.1016/j.saa.2010.04.021>
- ³⁸ S. Muthu, M. Prasath and R. Arun Balaji, *Spectrochim. Acta A: Mol. Biomol. Spectrosc.*, **106**, 129 (2013), <https://doi.org/10.1016/j.saa.2012.12.057>
- ³⁹ A. S. Kazachenko, N. Issaoui, O. Y. Fetisova, Y. D. Berezhnaya, O. M. Al-Dossary *et al.*, *Molecules*, **28**, 470 (2023), <https://doi.org/10.3390/molecules28020470>
- ⁴⁰ Q. Wang, N. Wang, W. Liu, Y. Yan, H. Su *et al.*, *ACS Sustain. Chem. Eng.*, **8**, 14353 (2020), <https://doi.org/10.1021/acssuschemeng.0c03934>
- ⁴¹ P. Politzer, P. R. Laurence and K. Jayasuriya, *Environ. Health Persp.*, **61**, 191 (1985), <https://doi.org/10.1289/ehp.8561191>
- ⁴² P. Politzer, J. S. Murray and F. A. Bulat, *J. Mol. Model.*, **16**, 1731 (2010), <https://doi.org/10.1007/s00894-010-0709-5>
- ⁴³ G. Venkatesh, C. Kamal, P. Vennila, M. Govindaraju, Y. S. Mary *et al.*, *J. Mol. Struct.*, **1171**, 253 (2018), <https://doi.org/10.1016/j.molstruc.2018.06.001>
- ⁴⁴ F. A. Bulat, A. Toro-Labbé, T. Brinck, J. S. Murray and P. Politzer, *J. Mol. Model.*, **16**, 1679 (2010), <https://doi.org/10.1007/s00894-010-0692-x>
- ⁴⁵ J. S. Murray, J. M. Seminario, P. Politzer and P. Sjöberg, *Int. J. Quantum Chem.*, **38**, 645 (1990), <https://doi.org/10.1002/qua.560382462>
- ⁴⁶ A. P. Karmanov, M. M. Ishankhodzhaeva and O. Y. Derkacheva, *Russ. Chem. Bull.*, **66**, 643 (2017), <https://doi.org/10.1007/s11172-017-1785-9>
- ⁴⁷ H. L. Hergert, *J. Org. Chem.*, **25**, 405 (1960), <https://doi.org/10.1021/jo01073a026>

- ⁴⁸ A.-A. M. A. Nada, M. A. Yousef, K. A. Shaffei and A. M. Salah, *Polym. Degrad. Stabil.*, **62**, 157 (1998), [https://doi.org/10.1016/S0141-3910\(97\)00273-5](https://doi.org/10.1016/S0141-3910(97)00273-5)
- ⁴⁹ M. L. Roldan, S. A. Centeno, A. Rizzo and Y. van Dyke, *MRS Online Procs. Libr.*, **1656**, 15 (2014), <https://doi.org/10.1557/opl.2014.823>
- ⁵⁰ J. Zhuang, M. Li, Y. Pu, A. J. Ragauskas and C. G. Yoo, *Appl. Sci.*, **10**, 4345 (2020), <https://doi.org/10.3390/app10124345>
- ⁵¹ R. H. Ellerbrock and H. H. Gerke, *J. Plant Nutr. Soil Sci.*, **184**, 388 (2021), <https://doi.org/10.1002/jpln.202100056>
- ⁵² V. Țucureanu, A. Matei and A. M. Avram, *Crit. Rev. Anal. Chem.*, **46**, 502 (2016), <https://doi.org/10.1080/10408347.2016.1157013>
- ⁵³ M. J. Baker, J. Trevisan, P. Bassan, R. Bhargava, H. J. Butler *et al.*, *Nature Prot.*, **9**, 1771 (2014), <https://doi.org/10.1038/nprot.2014.110>
- ⁵⁴ A. S. Kazachenko, E. Tanış, F. Akman, M. Medimagh, N. Issaoui *et al.*, *Molecules*, **27**, 7864 (2022), <https://doi.org/10.3390/molecules27227864>
- ⁵⁵ L. M. Lepodise and R. Bosigo, *Spectrochim. Acta A: Mol. Biomol. Spectrosc.*, **267**, 120469 (2022), <https://doi.org/10.1016/j.saa.2021.120469>
- ⁵⁶ A. V. Levdansky, N. Y. Vasilyeva, A. A. Kondrasenko, V. A. Levdansky, Y. N. Malyar *et al.*, *Wood Sci. Technol.*, **55**, 1725 (2021), <https://doi.org/10.1007/s00226-021-01341-2>
- ⁵⁷ J.-L. Wen, S.-L. Sun, B.-L. Xue and R.-C. Sun, *Materials*, **6**, 359 (2013), <https://doi.org/10.3390/ma6010359>
- ⁵⁸ R. Singh, V. Srivastava, K. Chaudhary, P. Gupta, A. Prakash *et al.*, *Bioresour. Technol.*, **188**, 280 (2015), <https://doi.org/10.1016/j.biortech.2015.01.001>
- ⁵⁹ N. Nićiforović, T. Polak, D. Makuc, N. Poklar Ulrih and H. Abramović, *Molecules*, **22**, 375 (2017), <https://doi.org/10.3390/molecules22030375>